



## Microbial analysis and parametric optimization of activated sludge process in paper and pulp mill effluent plant: a case study

N. Raggul<sup>a</sup>, R. Saraswathi<sup>b,\*</sup>

<sup>a</sup>Department of Civil Engineering, Anna University, Chennai, India, email: [ragguln@gmail.com](mailto:ragguln@gmail.com)

<sup>b</sup>Department of Civil Engineering, Coimbatore Institute of Technology, Coimbatore, India, email: [saraswathi70@rediffmail.com](mailto:saraswathi70@rediffmail.com)

Received 15 November 2014; Accepted 19 May 2015

---

### ABSTRACT

Environmental factors affecting the degradation efficiency of paper and pulp mill wastewater were identified and optimized in this study. An attempt has been made to design the thickening area of the secondary clarifier for paper and pulp mill wastewater to ensure critical loading condition by considering the initial concentration of mixed liquor suspended solids, recycling ratio, desired underflow concentration, and mean cell residence time. Natural coagulants, coagulant dose, and coagulant aid dose used in the coagulation-flocculation process were optimized using the design of experiment approach for turbidity and chemical oxygen demand reduction. Operational charts were developed for parameter adjustments in steady state process control.

*Keywords:* Paper and pulp mill; Secondary clarifier; Grey relational analysis; Bioremediation; Coagulation-flocculation; Physicochemical parameters; ANN; Operational diagram

---

### 1. Introduction

Pulp and paper mill effluent contains a large amount of organic matter which is a source of food for microorganisms. Wastewater treatment plants (WWTPs) based on the activated sludge process are subjected to transient operating conditions. The effective settling of activated sludge from the treated mixed liquor is mainly dependent on the ability of the activated sludge to form flocs. The activated sludge must be settled and separated from the treated water before it is discharged into any receiving water body. The activated sludge process is commonly used for secondary biological treatment to achieve very high efficiency of removal of

biochemical oxygen demand (BOD) and chemical oxygen demand (COD).

The function of a clarifier is to thicken the solids and return them to the aeration process. When this does not happen, the biological mass in the aeration basin ultimately decreases during the activated sludge process. Thus, the functions of the biological process and that of the secondary settling tank influence each other and the design of one cannot be undertaken independently of the other. Failure in either of these two unit processes causes failure of design objectives.

#### 1.1. Background and motivation

With an emphasis on sustainable wastewater treatment all over the world, many industries are keen

---

\*Corresponding author.

on pursuing methods that can be cost-effective and provide sustainable, long-term solutions for the treatment of wastewater [1]. Paper and pulp mills are sources of major pollution as they generate and release huge amounts of intensely colored effluents into the receiving end. Hence, paper industries are keenly exploring bioremediation as an important route to clean up wastewater [2,3]. Bioremediation uses naturally occurring microorganisms and other aspects of the natural environment to rid wastewater of its pollutants [4,5]. Such an approach provides an economical and environmentally sustainable way to treat wastewater. However, control measures are necessary to counter the colonization of microorganisms in paper mills, especially when white-water systems are being closed to reduce water consumption [6]. Efficient performance of a biological treatment unit depends on developing a suitable mixed culture of microorganisms in the aeration tank, by maintaining appropriate environmental conditions in the system. This study describes the interaction between the aerator and the secondary clarifier for the efficient functioning of an activated sludge system for treating paper and pulp mill wastewater. Coagulation-flocculation studies were conducted using natural coagulants to reduce the pollution load in aeration tank. With the optimal combination of microorganisms and optimized environmental parameters, settling studies were conducted at stationary phase to design the secondary clarifier of the WWTP.

## 2. Related work

Most soluble components from wood and recycled paper are biodegradable; therefore, biological treatment can efficiently reduce nutrients such as phosphorus, nitrogen, and multivalent metal ions [7]. Microbial species play a significant role in bio-oxidation and subsequent clarification in an activated sludge process. Microorganisms, such as bacteria, fungi, protozoa, and rotifers, exist in the activated sludge reaction vessel and clarifier as flocs. Microorganisms have developed a number of mechanisms enabling them to survive rather long periods without external substrates, some of which are still unknown [8]. Lerner et al. conducted experiments on aerobic and anaerobic versus aerobic bio-treatment of paper mill wastewater [9]. They compared the results from a full-scale activated sludge treatment (AST) system working as the only bio-treatment with those from an AST working with anaerobic pretreatment by up-flow anaerobic sludge blanket. Their findings indicate that

the anaerobic process, followed by AST, considerably reduced electrical and chemical consumption as well as the operational cost in the biological treatment plant. Much research has been done on natural coagulants such as cactus (*Cactaceous opuntia*) by Zhang et al. [10], *Moringa oleifera* by Ndabigengesere et al. [11], and *Ipomoea dasysperma* seed gum by Sanghi et al. [12]. Numerous studies have shown that *M. oleifera* seeds possess effective coagulation properties [13] and are not toxic to humans or animals. Chitosan is a natural cationic polyelectrolyte, a suitable coagulant for the treatment of industrial wastewater because it is safe and has no environmental impact. It has been used to treat olive oil wastewater [14] and pulp and paper wastewater [15].

This study focused on treating paper and pulp mill wastewater to bring down the pollution load by applying the above-mentioned techniques and methodologies. The study was planned in such a way that the operational parameters were optimized in each stage of the treatment process to ensure cost-effective functioning of the WWTP and so that its treatment efficiency could be more reliable. Empirical models were developed using the experimental data to optimize the operational parameters, and the results were validated using various optimization techniques such as response surface methodology (RSM) [16], artificial neural network (ANN) [17], and grey theory-based Taguchi method [18]. Using these models, plant operators will be able to assess the performance of paper and pulp effluent treatment.

## 3. Research approach

A brief overview of the methodology employed in this study is shown in Fig. 1. Phase-I shows the existing primary treatment practice in the paper and pulp mill, which is the subject of this study. Phase-II portrays the proposed optimization techniques for treating the paper and pulp mill wastewater to minimize the pollution load and maximize the efficiency of subsequent stages of treatment. Some of the processing needs in most WWTPs include improved performance as well as the minimization of operational costs and environmental impact while adhering to stringent standards for the process effluents. Optimization of every stage of the WWTP demands systematic investigation of each stage and the determination of control strategies [19] that will lead to minimization of multiple objective criteria.

This study was executed by employing the methodology mentioned below:

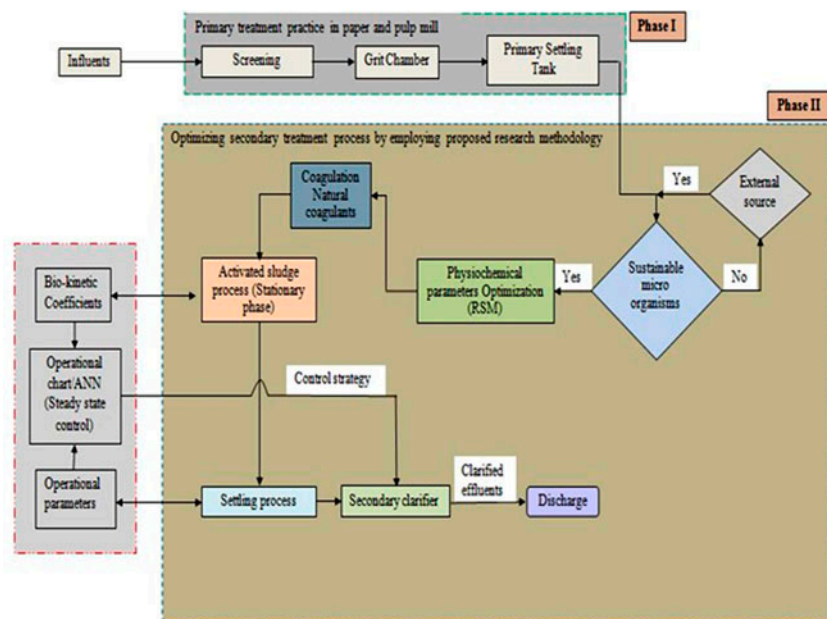


Fig. 1. Schematic diagram of research methodology.

- (1) Identifying the microorganisms present in paper and pulp mill effluent using biochemical methods.
- (2) Evaluating the effects of environmental factors such as temperature, pH, and incubation period on microbial survival and on physicochemical parameters.
- (3) Identifying optimal conditions for the use of natural coagulants in the coagulation\_flocculation processes for the removal of COD, total dissolved solids (TDS), and turbidity via the grey-based Taguchi method, thereby reducing the pollution load to the aeration tank.
- (4) Conducting column settling studies to design a secondary clarifier area and modeling the clarifier area using ANN.
- (5) Determining bio-kinetic coefficients on a laboratory scale in a continuous flow stirred tank reactor to develop an operational chart for the secondary clarification of activated sludge based on the solids flux theory using ANN.

### 3.1. Materials and methods

The effluent was obtained from a South India-based Integrated Pulp and Paper company. The paper pulp effluents from the outlet of the primary settling tank were used for the investigation. Samples were collected using sterile plastic containers and transported to the research laboratory within 4 h. The

effluent was stored at 4°C until required. All the testing was performed according to standard microbiological methods for the examination of water and wastewater [20]. The shake flask method was used to evaluate the treatment efficiency of individual isolates and also of combinations of isolates.

#### 3.1.1. Enumeration of bacteria

One milliliter of the raw effluent was added to 99 mL of sterile distilled water ( $10^{-1}$  L). The sample was serially diluted  $10^{-1}$ – $10^{-8}$  times using sterile pipettes. Nutrient agar medium containing peptone (5 g/L), yeast extract (1.5 g/L), sodium chloride (5 g/L), and agar (15 g/L) was sterilized before use for the enumeration of bacteria. The serially diluted samples ( $10^{-5}$  and  $10^{-6}$ ) were plated on nutrient agar plates, and the plates were incubated at 37°C for 24 h to obtain pure cultures (Fig. 2). The serially diluted effluent was

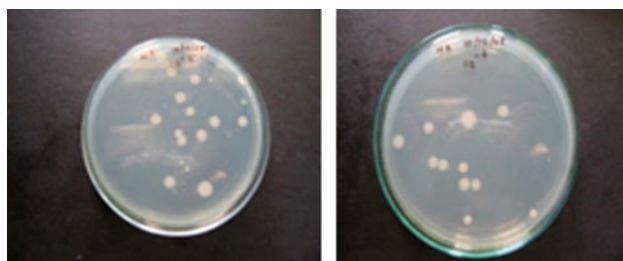


Fig. 2. Enumeration of bacteria ( $10^{-5}$  and  $10^{-6}$  dilution).

found to contain  $130 \times 10^{-5}$  colony-forming units (CFU)/mL and  $12 \times 10^{-6}$  CFU/mL of bacteria.

### 3.1.2. Enumeration of fungi

Potato dextrose agar medium containing potato (200 g), dextrose (20 g), agar (15 g), and distilled water (1,000 mL) at pH 5.6 was sterilized before use. The serially diluted samples ( $10^{-5}$  and  $10^{-6}$ ) were plated on potato dextrose agar plates, and the plates were incubated at room temperature for 3–5 d (Fig. 3). The serially diluted effluent was found to contain  $3 \times 10^{-5}$  and  $2 \times 10^{-6}$  CFU/mL of fungi.

### 3.2. Isolation and identification of organisms

The larger colonies appearing after the preliminary isolation were sub-cultured and subjected to identification. Five different organisms with different colony morphology were isolated by streaking on nutrient agar plates. The organisms were purified by repeated streaking on nutrient agar plates. Organisms were identified based on colony morphology, microscopic

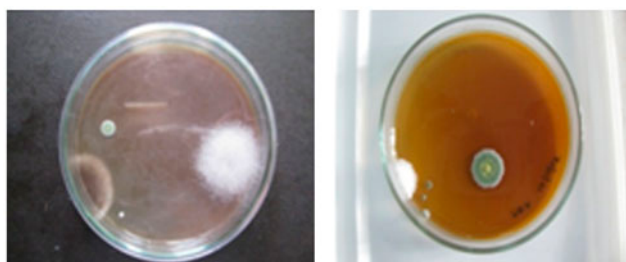


Fig. 3. Enumeration of fungi ( $10^{-5}$  and  $10^{-6}$  dilution).

observation, and confirmation tests. Gram staining was performed to distinguish between gram-positive and gram-negative bacteria under the microscope.

### 3.2.1. Microbial treatment of effluent

Raw effluent was treated with the isolated bacteria and fungi. Treatment efficiency was validated by calculating percent reduction of the physiochemical parameters. Table 1 gives the treatment efficiency of the five isolates; isolates of *Klebsiella* sp. and *Proteus* sp. were excluded from further study as their percent reduction of parameters were low compared to the other three isolates.

### 3.2.2. Combinations of microorganisms to improve treatment efficiency

To improve the efficiency of the bacterial treatment, the three isolates that were found to be good degraders were combined in different ways, as shown in Table 2, and a validation test was performed based on the same physiochemical parameters. It is evident from Table 2 that combinations 2 and 4 were found to be efficient when compared to other combinations; hence, they were used for further study.

Combination 1: *Pseudomonas alkaligenes* + *Bacillus pumilus*.

Combination 2: *P. alkaligenes* + *Bacillus subtilis*.

Combination 3: *B. pumilus* + *B. subtilis*.

Combination 4: *P. alkaligenes* + *B. pumilus* + *B. subtilis*.

*Trichoderma reesei* was found to be efficient in the treatment of paper mill effluent [21]. Hence, the

Table 1  
Treatment efficiency of individual bacteria

Parameters studied	% Reduction				
	<i>Pseudomonas alkaligenes</i>	<i>Bacillus pumilus</i>	<i>Bacillus subtilis</i>	<i>Klebsiella</i> sp.	<i>Proteus</i> sp.
pH*	7.3	7.5	7.5	7.1	7.8
TDS	11	12	12	0	11
TSS	58	60	59	35	20
BOD	92	79	85	60	55
COD	77	69	72	65	50
Hardness	40	58	47	23	0
Chlorides	36	32	29	11	11
Floc size	1 mm	2 mm	1.3 mm	0*	0*

Notes: pH\*—not in percentage; 0\*—no floc formation.

Table 2  
Treatment efficiency of different combinations of microorganisms

Parameters studied	% Reduction			
	Combination: 1	Combination: 2	Combination: 3	Combination: 4
pH*	7.3	7.3	8	7.7
TDS	11	12	0	11
TSS	49	58	42	49
BOD	77	98	69	62
COD	59	77	66	69
Hardness	39	45	40	40
Chlorides	36	36	36	36
Floc size	0*	1.2 mm	0*	1.1 mm

Notes: pH\*—not in percentage; 0\*—no floc formation.

efficient bacterial combination 2 (*P. alkaligenes* + *B. subtilis*), combination 4 (*P. alkaligenes* + *B. pumilus* + *B. subtilis*), and *T. reesei* were combined to enhance the treatment efficiency even further. It is evident from Table 3 that combination 2 + *T. reesei* was more efficient than combination 4 + *T. reesei*, and the derived consortia were used for the validation and the standardization of process parameters.

### 3.3. Effects of temperature and pH on physicochemical parameter reduction

The characterization of paper mill effluent and culture preparation of the sample effluent was carried out as discussed in the preceding Sections 3.1 and 3.2. Among the identified microorganisms, two bacterial strains and one fungal strain were found to be more efficient during the preliminary study; therefore, further investigations were continued with these three microorganisms only. The identified bacteria (*Pseudomonas*, *Bacillus* types) and fungal colonies

(*Trichoderma*) were used to determine the efficiency of degradation of the paper and pulp mill effluent under various temperature and pH conditions. Degradation studies were performed in paper and pulp mill effluent in batch shake flasks in an orbital shaker at 100 rpm.

The study was performed in two phases as described by Saraswathi and Saseetharan [22]. The impact of temperature variation in degradation rate was analyzed in the first phase at temperatures ranging from 25 to 55°C at intervals of 10°C. In the second phase, the effect of pH was assayed using 1 N NaOH in a pH range of 3–9. Degradation was carried out at 25, 35, 45, and 55°C, and the optimal temperature was established for floc permanence. Saraswathi and Saseetharan [21] had already described the influence of temperature on floc stability in an earlier study. The results obtained from the central composite design (CCD) experiments were fitted to a second-order polynomial equation to explain the dependence of microbial degradation on medium components.

Table 3  
Treatment of effluent using the bacterial and fungal isolates

Parameters studied	% Reduction	
	Combination: 2 + <i>T. reesei</i>	Combination: 4 + <i>T. reesei</i>
pH*	7.2	6.9
TDS	22	12
TSS	59	52
BOD	99	82
COD	85	72
Hardness	56	40
Chlorides	40	36
Floc size	1.7 mm	1.2 mm

Note: pH\*—not in percentage.

Statistical analysis proved that the interaction effects between pH and temperature, pH and time ( $P \approx 0.9$ ) for TDS and BOD; and temperature and time ( $P \approx 0.7$ ) for BOD, COD, and chlorides were found to be significant. The significance of these interaction effects between the variables would have been lost if the experiments were carried out by conventional methods. A mathematical model using MINITAB 14 software was used in the above study to generate the optimal values for the above three variables. The model-predicted values for the rate of decrease in physiochemical parameters from the experimental study were found to be 5.37% TDS, 45.37% TSS, 73.87% BOD, 63.98% COD, 32.59% hardness, 17.59% chlorides, and floc size of 1.16 mm, which is nearly 75% of the degradation seen under optimized conditions. Optimization results from RSM show that a more marked decrease in physiochemical parameters can be achieved with some modification in the physical parameters (pH, temperature, and incubation period), thus enhancing degradation as well.

### 3.4. Coagulation\_flocculation process

Coagulation is the most widely used process in wastewater treatment and is usually achieved through the addition of inorganic coagulants, such as aluminium or iron-based salts, and/or synthetic organic polymers commonly known as polyelectrolytes [23]. Coagulation involves the precipitation of flocs that adsorb and remove pollutants. This method is used for the removal of metals, treatment of toxic wastes, removal of turbidity and suspended solids, and the control of color. Thus, it is economical and enhances the effectiveness of subsequent treatments [24]. This experimental study explored the optimal conditions of the coagulation\_flocculation process in paper mill wastewater treatment by employing the Taguchi method and grey relational analysis (GRA) by Saraswathi and Saseetharan [18]. Coagulation\_flocculation experiments were carried out in a jar test apparatus (OSK—Japan). After thorough mixing, the wastewater was allowed to settle for 2 h and the supernatant was collected and transferred to a clean container. Precise dosages of coagulants, including *M. oleifera*, *Vicia faba*, Bentonitic clay, *Pisum sativum*, and of coagulant aids including calcium carbonate, ferric chloride, aluminium sulfate, ammonium sulfate, were added to 1,000-mL jars containing paper and pulp mill wastewater with specific pH values. A series of jar tests were carried out by rapid mixing followed by slow mixing. The rapid mixing was carried out at 100 rpm for 3 min followed by slow mixing at 30 rpm

for 25 min. Finally, the aggregated particles were allowed to settle for 30 min after coagulation\_flocculation. The resulting supernatants were used for the measurement of the remaining COD, TSS, TDS, and turbidity.

GRA based on Taguchi method was used to evaluate the feasibility of using coagulation\_flocculation process in paper and pulp mill wastewater treatment. Optimal coagulation\_flocculation process parameters have been determined by grey relational grade (GRG) for multi-performance characteristics (COD, TDS, and turbidity). From the response table of average GRG values, the following parameters showed maximum GRG values for: coagulant aid dose, 120 ppm; coagulant aid type,  $\text{Al}_2(\text{SO}_4)_3$ ; pH 9; coagulant dose, 500 ppm; and coagulant type, *V. faba*. These are the recommended levels of controllable process parameters when larger COD and TDS values as well as lower turbidity levels are simultaneously attained. ANOVA of GRG for multi-performance characteristics revealed that the coagulant aid dose is the most significant parameter. Based on the confirmation test, improvements in performance characteristics were as follows: COD removal is 8.2%, TDS removal is 6.35%, and turbidity removal is 26.1%. Thus, performance characteristics of coagulation\_flocculation process parameters are simultaneously improved using GRA. This study was performed to bring down the pollution load in the effluent being fed to the aeration tank.

## 4. Design of secondary clarifier

The secondary settling tank plays a very crucial role in achieving very strict effluent standards of wastewater treatment plants. The principal function of secondary settling tanks is to separate the activated sludge from the biologically treated wastewater. The loading capacity of an activated sludge plant is determined substantially by the concentration of suspended solids in the activated sludge and the volume of the aeration tank. The concentration of suspended solids depends essentially on the functional capacity of the secondary settling tanks with fluctuating hydraulic feeding, sludge volume index, sludge removal as well as the return sludge ratio and waste sludge removal.

### 4.1. Experimental system

Experiments were carried out in a bench scale reactor. Two air pumps with normal air flow rates were used for air supply. The air pump was connected with four stone diffusers and a horizontal diffuser for complete aeration to keep the contents of

the reactor in a completely mixed regimen. A glass heater (Amazon, 220 V, temperature range 20–50 °C) was used to maintain the temperature in the reactor. A glass settling column of 600 mm height and 22.5 mm diameter was used for settling studies. Settling studies were conducted in stationary phase for mean cell residence times ( $\theta_c$ ) of 5, 7, 9, 11, and 13 d.

#### 4.1.1. Activated sludge preparation

Dilution experiments were carried out for paper and pulp mill sludge by running a batch scale reactor in stationary phase. The reactor was filled with 20 L of the effluent (primary outlet), 5% of the activated sludge seeding, and 5% of the inoculum containing isolates of *Bacillus subtilis*, *P. alkaligenes*, and *T. reesei* isolated from the sludge seeding. Factors such as pH and temperature were optimized for these microbes by conducting laboratory-scale experiments. The microbes showed effective reduction in parameters such as hardness, chlorides, COD, BOD, and TDS at 35 °C and pH 7. Temperature stabilization was done using the glass heater, and pH stabilization was done manually using 0.1 N HCl and 0.1 N NaOH. The mixture was aerated continuously using a diffused aeration system to keep the mixture in a completely mixed state and to supply oxygen to the aerobic bacteria. The units were operated with  $\theta_c$  ranging from 5 to 13 d in the stationary phase of microbial growth after the acclimatization and stabilization period. The daily loading rate was based on food to microorganism ratio (F/M) of 0.25 kg BOD/kg mixed liquor volatile suspended solids (MLVSS) for the stationary phase [25,26]. From the time of inoculation of the microbes into the system, parameters like COD, hardness, chlorides, pH, and TDS were monitored for every 24 h until steady state was reached. Microbial counting was done by serial dilution and spread plating methods to estimate microbial growth with respect to the availability of substrates (organic/inorganic content) in the effluent.

#### 4.2. Performing settling studies

Settling studies were conducted for mixed liquor suspended solids (MLSS) from 2 to 8 g/L with an increment of 1 g/L and from 8 to 20 g/L with an increment of 2 g/L for mean cell residence times ( $\theta_c$ ) of 5, 7, 9, 11, and 13 d. The desired  $\theta_c$  was maintained by wasting a portion of mixed liquor ( $\theta_c = V/Q_w$ ) from the reactor manually. Interface height was monitored for 90 min. Fig. 4 shows the settling curve for

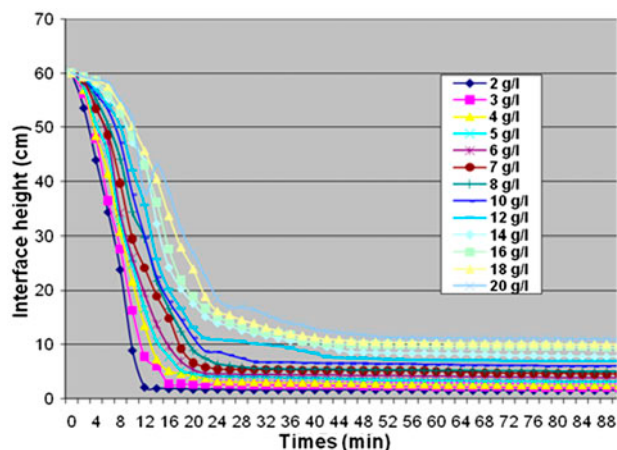


Fig. 4. Settling curve for  $\theta_c = 5$  d.

$\theta_c = 5$  d for different MLSS levels. Similar settling curves for different MLSS and  $\theta_c$  values were developed in stationary phase for  $\theta_c = 7, 9, 11,$  and 13 d. Through experience, operators of conventional activated sludge reactors have found that  $\theta_c$  should lie between 3 and 14 d in order to produce a biological floc that can be handled easily. The settling characteristics of activated sludge depend upon the physiological state of the organisms present, which is controlled by regulating the MCRT.

#### 4.3. Zone settling velocity

Interface height versus time is a linear function. Zone settling velocity associated with a particular concentration can be determined as the slope of the linear part of the settling curve [26]. Zone settling curves for  $\theta_c = 5, 7, 9, 11, 13$  d are shown in Fig. 5. It was observed that the zone settling velocity increases with increase in  $\theta_c$  and decreases with an increase in MLSS concentration. This is because at higher MLSS concentrations, the likelihood for particles to approach each other is higher due to which the inter-particle forces are higher, thus decreasing the rate of settling of the sludge particle by Chen et al. [27]. Dupont and Henze [28] reported that the settling velocity in a zone settling model is assumed to depend on the gravity forces acting on the particles and on the inter-particle forces only. This means that the settling velocity decreases downwards through the clarifier with increasing sludge concentration. Sludge age values would result in high removal efficiencies. Operation with high sludge age renders the system capable of assimilating shock loads without affecting sludge settleability [25].

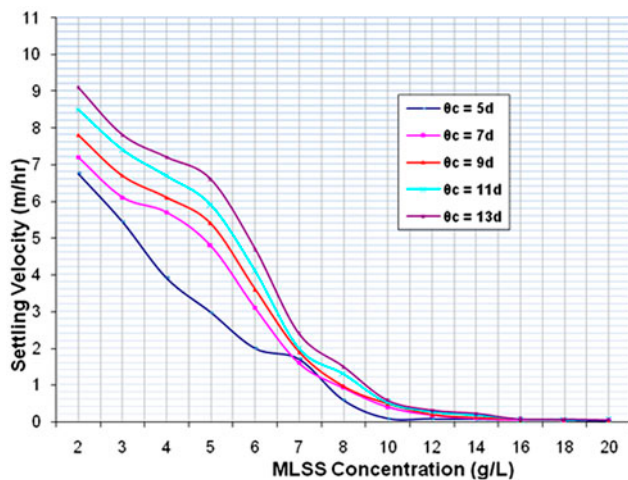


Fig. 5. Zone settling curve.

#### 4.4. Solid flux analysis

Solids flux is defined as the mass of sludge solids passing through a unit horizontal area in a unit time. The area required for thickening of the applied mixed liquor depends on the limiting solids flux that can be transported to the bottom of the sedimentation tank. As the solids flux varies with the characteristics of the sludge, column settling tests should be conducted to determine the relationship between the sludge concentration and the settling rate. As the sludge concentration usually has to pass through the critical concentration which defines maximal solid loading, the design of the secondary settling tank is based essentially on the estimation of the required area for that value of the limiting flux,  $G_L$ . Gravity flux curves were developed for  $\theta_c = 5, 7, 9, 11, 13$  d at stationary phase (Fig. 6).

The equations derived from material balance were used for calculating  $C_0$  and  $A/Q$  for any values of  $C_w$ ,  $G_L$ ,  $R$ . Table 4 shows the calculated values of  $A/Q$  and  $C_0$  at different recycle ratios for  $\theta_c = 5$ . Similarly, the values for  $A/Q$  and  $C_0$  at different recycle ratios for  $\theta_c = 7, 9, 11, 13$  were obtained from experiential studies.

The following inferences were drawn from the settling studies:

When  $\theta_c$  increases, the surface charge on microbial cells is reduced as the zone settling velocity increases. The microorganisms start to produce extracellular enzymes and eventually become encapsulated in a slimy layer. Formation of this slimy layer promotes floc formation and enhances the rate of gravity settling. Fig. 6 shows the effect of mean cell residence time on the settling nature of activated sludge

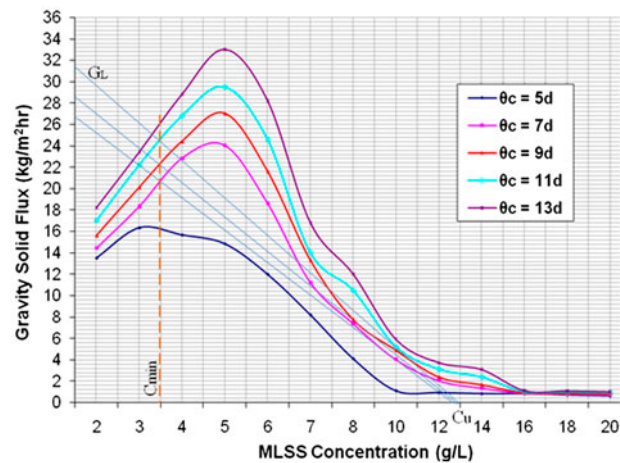


Fig. 6. Gravity solid flux curves.

suspensions. The fitted curves obtained for the effects of sludge age on zone settling velocity show that greater sludge age resulted in higher removal efficiencies. When zone settling velocity increases with increase in mean cell residence time, the limiting solid flux also increases. This in turn reduces the value of  $A/Q$  and the surface area requirement of the secondary clarifier. Moreover, waste is completely mineralized at longer  $\theta_c$ .

### 5. Performance evaluation of ETP using ANN model

Neural networks (NNs) have been widely used for complex processes that are poorly described by first principle models, such as wastewater biological treatment systems. In recent years, NNs have been successfully applied to various biochemical processes [29,30]. They have a distinct ability to model nonlinear dynamic systems without requiring a structural knowledge of the process to be modelled. NNs can map a set of input patterns onto a corresponding set of output patterns on the basis of historical data. In this section, an artificial NN (ANN)-based predictive model has been proposed to assess the performance of paper and pulp effluent treatment plants. In this study, recirculation ratio ( $R$ ), underflow concentration ( $C_w$ , g/L), and limiting solid flux ( $G_L$ , kg/m<sup>2</sup> h) were selected as input variables. Area of secondary clarifier required per unit flow ( $A/Q$ ) was selected as the output variable.

There are two important stages in ANN-based model development: The first stage is training the model and the second stage is testing of the trained model. Training of an ANN requires input data, namely  $R$ ,  $C_w$ , and  $G_L$ . The parameters  $R$ ,  $C_w$ ,  $C_0$ , and

Table 4  
 $A/Q$  values for  $\theta_c = 5$  d

$C_u$ (g/L)	$G_L$ (kg/m <sup>2</sup> h)	Description	Recycle ratio					
			0.25	0.40	0.55	0.70	0.85	1.00
10	20.7	$C_0$	2	2.9	3.5	4.1	4.6	5
		$A/Q$	0.121	0.193	0.265	0.338	0.41	0.483
11	11.65	$C_0$	2.2	3.19	3.85	4.51	5.06	5.5
		$A/Q$	0.236	0.377	0.519	0.66	0.802	0.944
12	6.7	$C_0$	2.4	3.48	4.2	4.92	5.52	6
		$A/Q$	0.5	0.716	0.985	1.27	1.52	1.79
13	4.65	$C_0$	2.6	3.77	4.55	5.33	5.98	6.5
		$A/Q$	0.698	1.18	1.537	1.95	2.37	2.79
14	3.9	$C_0$	2.8	4.06	4.9	5.74	6.44	7
		$A/Q$	0.897	1.435	1.97	2.51	3.05	3.5
15	3.2	$C_0$	3	4.35	5.25	6.15	6.9	7.5
		$A/Q$	1.17	1.875	2.578	3.28	3.98	4.68
16	2.8	$C_0$	3.2	4.64	5.6	6.56	7.36	8
		$A/Q$	1.43	2.285	3.14	4	4.85	5.71
17	2.5	$C_0$	3.4	4.93	5.95	6.97	7.82	8.5
		$A/Q$	1.7	2.72	3.74	4.76	5.78	6.8
18	2.4	$C_0$	3.6	5.22	6.3	7.38	8.28	9
		$A/Q$	1.87	3	4.125	5.25	6.375	7.5
19	2.2	$C_0$	3.8	5.51	6.65	7.79	8.74	9.5
		$A/Q$	2.16	3.45	4.75	6.04	7.34	8.63
20	2.1	$C_0$	4	5.8	7	8.2	9.2	10
		$A/Q$	2.38	3.8	5.23	6.66	8.09	9.55
21	2	$C_0$	4.2	6.09	7.35	8.61	9.66	10.5
		$A/Q$	2.625	4.2	5.775	7.35	8.925	10.5
22	1.9	$C_0$	4.4	6.38	7.7	9.02	10.12	11
		$A/Q$	2.89	4.63	6.36	8.1	9.84	11.57
23	1.85	$C_0$	4.6	6.67	8.05	9.43	10.58	11.5
		$A/Q$	3.11	4.97	6.837	8.7	10.56	12.43
24	1.75	$C_0$	4.8	6.96	8.4	9.84	11.04	12
		$A/Q$	3.43	5.48	7.52	9.6	11.65	13.71

$A/Q$  were correlated so as to develop the model for the thickener area of secondary settling tank. The models were developed for various  $\theta_c$  (5–13 d) and  $R$  (0.25–1.0) values. The primary goal of training is to minimize an error function by searching for a set of connection strengths and biases that cause the ANN to produce outputs that are equal or close to targets. The architecture, training method, and training rates were determined for the model using a trial and error approach. Training was stopped when there was no further improvement (reduction in root mean square error) in the forecasts obtained using an independent test dataset. This value, which is the model-predicted value, was compared to the correct value for the given patterns, and the connection weights were modified to decrease the sum of the squared error. The training records contain sufficient patterns to allow the ANN

model to adequately mimic the underlying relationships between the output and input variables. The test records were not applied to the networks during training, but they were used to test the performance of the trained network for its forecasting ability of output variables after the training was completed. Representative data for training and test data for the developing ANN model are given in Table 5.

The training time varied between 1.8 and 22 s (Table 6). Test data were applied to the network for each value of  $\theta_c$  and  $R$ . The simulation results obtained by the ANN coincided well with the experimental data. For a given value of  $\theta_c$  and different values of  $R = 0.25$ –1.0, the feed-forward NN was trained and the trained network was tested with the test data. Training specifications of the ANN model for  $\theta_c = 11$  d and  $R = 0.4$  are given in Fig. 7 from which it could be

Table 5  
Representative data for training and testing ANN model ( $\theta_c = 7$  d,  $R = 0.4$ )

Trial No.	ANN train data						ANN test data					
	$C_u$	$G_L$	$C_0$	$E$ (A/Q)	ANN (A/Q)	Error	$C_u$	$G_L$	$C_0$	$E$ (A/Q)	ANN (A/Q)	Error
1	10	29.1	2.86	0.1376	0.1375	1E-04	10.1	28.7	2.88	0.1407	0.1408	-0.0001
2	11	22.2	3.14	0.1982	0.1982	0	11.3	21.1	3.23	0.2142	0.2142	0
3	12	19.3	3.43	0.2486	0.2487	-0.0001	12.6	18.65	3.6	0.2792	0.2792	0
4	13	17.2	3.71	0.302	0.302	0	13.8	14	3.94	0.3942	0.3943	-1E-04
5	14	13.3	4	0.421	0.4211	-1E-04	14.1	13	4.03	0.4338	0.4338	0
6	15	10.4	4.29	0.576	0.5769	-0.0009	15.3	9.3	4.37	0.658	0.6581	-1E-04
7	16	8.1	4.57	0.79	0.7901	-1E-04	16.6	7.35	4.74	0.9034	0.9034	0
8	17	6.7	4.86	1.014	1.0149	-0.0009	17.8	6	5.09	1.1866	1.1867	-1E-04
9	18	5.9	5.14	1.22	1.2203	-0.0003	18.2	5.7	5.2	1.2771	1.2772	-1E-04
10	19	4.9	5.43	1.54	1.551	-0.011	19.4	4.55	5.54	1.7054	1.7055	-1E-04
11	20	4.1	5.72	1.948	1.95	-0.002	20.3	3.8	5.8	2.1368	2.1368	0
12	21	3.45	6	2.43	2.4348	-0.0048	21.8	2.8	6.23	3.1142	3.1143	-0.0001
13	22	2.7	6.29	3.25	3.2593	-0.0093	22.7	2.4	6.49	3.7833	3.7833	0
14	23	2.3	6.57	4	4	0	23.4	2.15	6.8	4.427	4.4279	-0.0009
15	23.5	2.2	6.7	4.2727	4.2727	0	23.6	2.1	6.83	4.5523	4.5524	-1E-04

determined that the error was 1E-5 and the training data required 139 epochs. Results were similarly obtained for the remaining ANN data.

The epochs required for the trained feed-forward network varied between 100 and 500. The accuracy of the results is in the range of 1E-3. ANN models were trained for each  $\theta_c$  of 5, 7, 9, 11, and 13 d and for the  $R$  values of 0.25, 0.4, 0.55, 0.7, 0.85, and 1.0. After all the data were trained, new sets of data were tested. Among the 4,230 data, 2,230 were used as training data and the remaining 2,000 as testing data. The computation of regression coefficient, i.e.  $R^2 = 0.992$  for the train data and test data was obtained from Minitab 16, which exhibits the robustness of the ANN model.

### 5.1. Evolution of the mathematical model

It should be noted that, theoretically, using an infinite number of independent variables to explain the change in a dependent variable would result in a high correlation coefficient ( $R^2$ ) of one for the modeling datasets. In contrast to  $R^2$ , the adjusted  $R^2$  increases only if the additional model parameters improve the regression results significantly to compensate for the increase in regression degree of freedom. Nevertheless, there is no similar statistical parameter to perform reliable comparative analyses of the predictive performances of NN models, and the methods proposed in the literature usually lead to contradictory results. Comparative analyses of statistical and NN models are based on  $R^2$  values estimated from the validation and test datasets. The quality of match

between the ANN model values and experimentally measured values was verified with the mathematical model using SPSS software (Ver.15.0). A mathematical model was obtained for the thickener area of secondary settling tank by correlating the parameters  $R$ ,  $C_u$ ,  $C_0$ , and  $A/Q$ .  $R^2$  shows the effectiveness of the models developed in this study. These models are depicted in (Eqs. (1)–(6)).

#### Mathematical model for experimental data

$$\log(A/Q) = -2.967 + 2.405 \log C_u + 1.505 \log C_0 - 1.097 \log \theta_c, R^2 = 0.917 \tag{1}$$

$$\log(A/Q) = -3.401 + 3.909 \log C_u + 1.000 \log R - 1.097 \log \theta_c, R^2 = 0.918 \tag{2}$$

$$\log(A/Q) = -2.245 + 3.881 \log C_0 + 1.568 \log R - 1.097 \log \theta_c, R^2 = 0.913 \tag{3}$$

#### Mathematical model for ANN data

$$\log(A/Q) = -3.018 + 2.553 \log C_u + 1.505 \log C_0 - 1.225 \log \theta_c, R^2 = 0.968 \tag{4}$$

$$\log(A/Q) = -3.452 + 4.058 \log C_u + 1.000 \log R - 1.225 \log \theta_c, R^2 = 0.969 \tag{5}$$

Table 6  
Training and simulation time for various MCRT ( $\theta_c$ )

MCRT (d)	R = 0.25		R = 0.40		R = 0.55		R = 0.70		R = 0.85		R = 1.0	
	Training time (s)	Simulation time (s)										
5	7.117237	0.01788	2.671431	0.011593	2.560292	0.017478	3.738856	0.013662	4.907897	0.013191	10.789640	0.013403
7	7.950571	0.093089	3.719618	0.013330	5.951715	0.016978	11.398533	0.096304	3.697090	0.011580	5.537524	0.012748
9	1.8966588	0.011831	4.704291	0.012899	1.947908	0.012900	9.590542	0.011016	7.7259905	0.013465	22.602292	0.010564
11	16.212307	0.136313	12.14948	0.142725	3.113203	0.010987	7.874811	0.014416	4.579651	0.14291	2.957643	0.016157
13	13.173632	0.012431	8.640731	0.009889	2.532787	0.013450	8.753423	1.075456	4.140551	0.011343	6.473655	0.016195

$$\log(A/Q) = -2.252 + 4.029 \log C_0 + 1.665 \log R - 1.225 \log \theta_c, R^2 = 0.964 \quad (6)$$

In this study, two models based on ANN and experimental investigations were developed to predict the area of the secondary clarifier for unit flow for a major paper and pulp mill WWTP. The ANN models provide a robust tool for prediction in which the prediction error varied slightly and smoothly over the range of data sizes used in training and testing. Once the feed-forward architecture for the training data was created, it could be utilized for identifying the  $A/Q$  value for any input data. The test data applied to the  $A/Q$  values coincided very well with the experimental values. ANN has proved to be a very useful tool in overcoming some of the limitations of conventional mathematical models for effluent treatment plants because of their complex mechanisms, variability, and dynamics. The secondary clarifier area can be designed using the models proposed in this study for any values of  $C_w$ ,  $C_0$ ,  $R$ , and  $\theta_c$ . The predicted models give a rational approach to the design of a secondary clarifier.

## 6. Steady state process control for activated sludge

The final settling tank is a vital part of the activated sludge process. It combines two functions, namely clarification and thickening. Failing to provide either of these two functions results in solids being carried over with the final effluent. This will not only affect the effluent quality, but can also affect the behavior of the biological process. In this study, operational charts for secondary clarification of activated sludge were developed to connect the process operational parameters, MLSS, flow, volume, area, and recycle ratio, in a unified graphical form. This chart can be used to design and analyze the performance of secondary clarification and to evaluate operating strategies in response to changes in flow rate or solid settleability.

### 6.1. Materials and method

Laboratory-scale reactors are normally used to determine kinetic coefficients. A completely mixed continuous flow reactor is usually employed without recycling for its easy operational control. In such a reactor, detention time ( $\theta$ ) is equal to the mean cell residence time ( $\theta_c$ ). The procedure is to operate the unit over a range of effluent substrate concentrations. Using the data collected at steady state conditions,

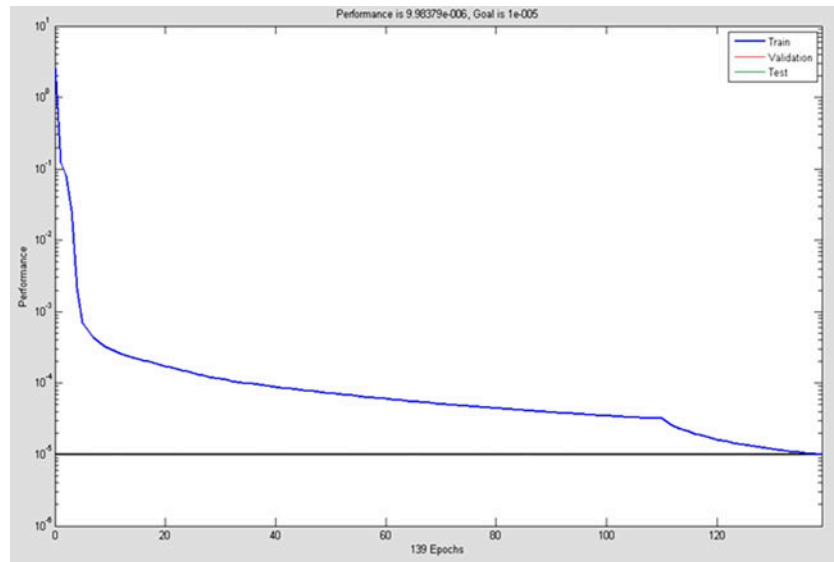


Fig. 7. Training specifications of ANN model for  $\theta_c = 11$  d,  $R = 0.4$ .

mean values are determined for influent BOD ( $S_o$ ), effluent BOD ( $S$ ), and MLSS of the aeration tank (denoted by  $X$ ) to determine the kinetic coefficients. The capacity of the influent tank was 18 L. The wastewater to the reactor was fed using a 20-L glass tank. A peristaltic pump was used to regulate the flow for a particular  $\theta_c$ . Diffuser stones were used to supply air and were placed at the bottom of the aeration tank along the wall. Filtered air was supplied to the diffuser stones from an air pump. A final clarifier of 10 L capacity followed the aeration tank.

### 6.2. Determination of kinetic coefficients

The purpose of studying kinetic coefficients is to obtain information on the rate of cell growth and the consumption of substrates. This enables the calculation of the required volume of the reactor, and the simulation of the system can be used for process control. Kinetic coefficients of a biological system have generally been determined experimentally using either continuous flow, completely mixed, or batch laboratory-scale reactors. In a continuous flow completely mixed reactor, kinetic coefficients are usually determined by collecting data from laboratory-scale or pilot-plant experiments. The system was operated at various hydraulic retention times or at various sludge retention times, and at steady state. Measurements of the biomass and permeate substrate concentration were recorded. Parameters such as  $K_s$ ,  $\mu$ ,  $Y$ , and  $k_d$  were determined through the linearization of equations. Mean values of the influent substrate concentration,

effluent substrate concentration, and MLSS concentration were measured to determine the kinetic coefficients for various mean cell residence times  $\theta_c = 5, 7, 9, 11,$  and  $13$  d (Table 7).

In order to determine the yield coefficient ( $Y$ ) and endogenous decay constant ( $K_d$ ), a graph (Fig. 8) was plotted with  $1/\theta_c$  on the  $y$ -axis and  $(S_o - S)/X$  on the  $x$ -axis. As there is no recycling in this experiment,  $\theta$  can be written as  $\theta_c$ . The slope of the line gives the yield coefficient, and the  $y$ -intercept gives the endogenous decay constant ( $K_d$ ). The value of the yield coefficient,  $Y$ , was 0.5 and the endogenous decay coefficient  $k_d$  was  $0.14 \text{ d}^{-1}$ .

Using these kinetic coefficients, the volume of the reactor can be calculated by Eq. (7)

$$V = \frac{YQ(S_i - S_c)}{X(1/\theta_c + k_d)} \quad (7)$$

where  $Y$  is the yield coefficient given by Eq. (8)

$$Y = \frac{r_{su}}{r_g} = \frac{\text{Substrate utilised}}{\text{Growth rate}} \quad (8)$$

### 6.3. Evolution of zone settling velocity constants

Batch settling studies were conducted for paper and pulp mill activated sludge for  $\theta_c = 5, 7, 9, 11, 13$  d in stationary phase, as discussed in Section 4.2. Zone settling velocity “ $v$ ” was determined for various  $C_0$  and  $\theta_c$  values in the stationary phase, as discussed in

Table 7  
Data for determining bio-kinetic coefficients

$\theta_c$ (d)	Mean $S_o$ (mg/L)	Mean $S$ (mg/L)	MLSS $X$ (mg/L)
5	386	203	145
7	326	149	106
9	282	123	86
11	379	91	153
13	328	64	139

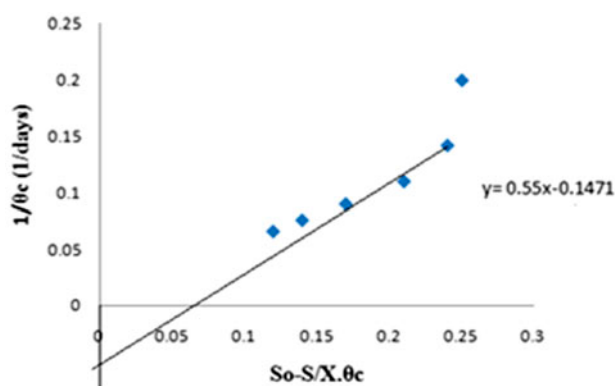


Fig. 8. Determination of kinetic coefficients.

Section 4.3. Control strategies were developed based on steady state control methods in the stationary phase. Steady state process control is used to control the performance of the activated sludge process subject to transient loading conditions for a long term on a rational basis. The values of zone settling velocity ( $v$ ) and concentration ( $C_0$ ) were analyzed for curve fitting. The model of best fit conforming to the available data of  $v$  and  $C_0$  was the exponential model,  $v = V_o e^{(-aC_0)}$ . The values of the constants  $a$  and  $V_o$  for  $\theta_c$  (5, 7, 9, 11, 13 d) for the stationary phase are represented in Table 8. Results show that the coefficient of  $V_o$  is not influenced by solid concentration, whereas “ $a$ ” has influence on solid concentration on the settling velocity.

Table 8  
Zone settling constants—stationary phase

$\theta_c$ (d)	$a$	$V_o$
5	0.3312	5.1853
7	0.2996	8.2173
9	0.2735	9.6643
11	0.2609	10.2626
13	0.2571	11.9504

Table 9a  
Values of  $(VX/A)$  for various  $S_i$  and  $(Q/A)$  for  $\theta_c = 5$  d (experimental)

$S_i \rightarrow Q/A \downarrow$	100	150	200	250	300	350	400
0.3	0.77	1.32	1.87	2.42	2.97	3.52	4.08
0.6	1.54	2.64	3.75	4.8	5.9	7.05	8.16
0.9	2.31	3.96	5.62	7.2	8.9	10.57	12.34
1.2	3	5.28	7.5	9.6	11.9	14.1	16.32
1.5	3.85	6.6	9.37	12	14.82	17.6	20.4
1.8	4.63	7.92	11.25	14.4	17.8	21.3	24.4

Table 9b  
Values of  $(VX/A)$  for various  $V$  and  $(X/A)$  for  $\theta_c = 5$  d (experimental)

$V \rightarrow X/A \downarrow$	200	400	600	800	1,000	2,000
0.01	2	4	6	8	10	20
0.02	4	8	12	16	20	40
0.03	6	12	18	24	30	60
0.04	8	16	24	32	40	80
0.05	10	20	30	40	50	100
0.06	12	24	36	48	60	120

Table 9c  
Values of  $X$  for various  $A$  and  $(X/A)$  for  $\theta_c = 5$  d (experimental)

$A \rightarrow X/A \downarrow$	50	100	150	200	300	400
0.01	0.5	1	1.5	2	3	4
0.02	1.0	2	3	4	6	8
0.03	1.5	3	4.5	6	9	12
0.04	2.0	4	6	8	12	16
0.05	2.5	5	7.5	10	15	20
0.06	3.0	6	9	12	18	24

Table 9d  
Values of  $(Q/A)$  for various  $C_0$  and  $R$  for  $\theta_c = 5$  d (experimental)

$R \rightarrow C_0 \downarrow$	0.20	0.30	0.40	0.50	0.6	0.7	0.8	0.9	1
2.00	2.67	2.67	2.67	2.67	2.67	2.67	2.67	2.67	2.67
3.00	1.2	1.9	1.9	1.9	1.9	1.9	1.9	1.9	1.9
4.00	0.8	1.29	1.4	1.4	1.4	1.4	1.4	1.4	1.4
5.00	0.59	0.9	1.08	1.14	1.2	1.29	1.29	1.29	1.29
6.00	0.47	0.63	0.8	0.87	0.98	1.03	1.1	1.1	1.2
7.00	0.24	0.58	0.53	0.63	0.75	0.88	0.97	0.97	1.08
8.00	0.07	0.35	0.39	0.48	0.57	0.71	0.85	0.92	1.02

6.4. Data generation and evolution of operational charts

Recognizing the need for a more easily applied approach for the design and analysis of the operational state of the secondary clarifier, operational charts were developed based on the experimental data determined through settling and kinetic studies by Antonio and Carbone [31]. Each operational chart has four quadrants. The first quadrant shows the relationship between  $Q/A$  and  $VX/A$  for  $S_i$  ranging from 100 to 400 mg/L. The second quadrant shows the relationship between  $VX/A$  and  $X/A$  for  $V$

ranging from 200 to 2,000  $m^3$ . The third quadrant relates the parameters  $X/A$  and  $X$  for different values of  $A$  ranging from 50 to 400  $m^2$ . The fourth quadrant shows the relationship between  $C_0$  and the overflow rate for various recycling ratios  $R$ , ranging from 0.2 to 1.0 for the stationary phase. For any change in  $Q/A$ , it is possible to find the value of  $R$  that satisfies the condition of the application of lower solid flux as compared to the limiting solid flux, and the adjusted  $R$  ensures the necessary  $C_0$  in the reactor. The lower part of the fourth

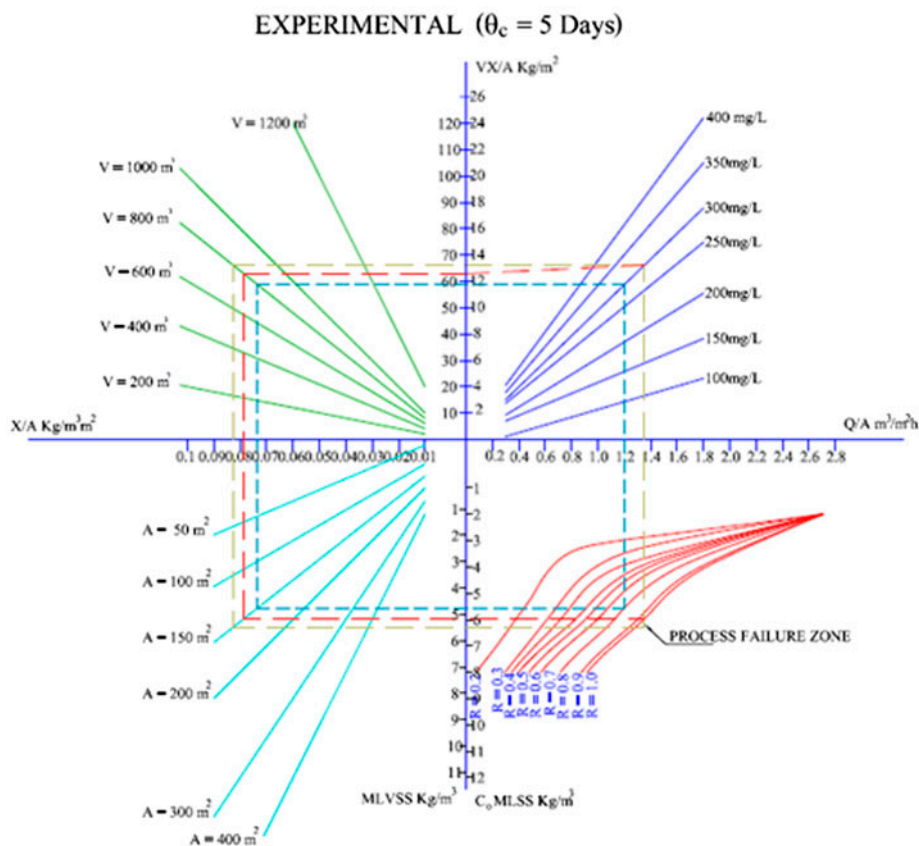


Fig. 9. Operational chart for  $\theta_c = 5$  d (experimental).

quadrant corresponds to the curve of the equation  $Q/A = V_0 \exp^{-a C_0}$ , which shows the region of failure. It is possible to adjust the recycling ratio  $R$  for maintaining the MLSS concentration in the reactor above this curve for any variation in the overflow rate. The lower part of the curve of the fourth quadrant shows that whatever the  $Q/A$ , no value of  $R$  gives the  $C_0$  value compatible with the proper functioning of the secondary clarifier. Each point in this area represents the failure of the system, which leads to the raising of the sludge blanket in the secondary clarifier and the presence of suspended solids in the final effluent. The data generated to draw the operational chart for various  $\theta_c = 5$  d in stationary phase are given in Tables 9a–9d, and the corresponding operational charts are shown in Fig. 9.

Similar diagrams can be drawn for the remaining  $\theta_c$  values

6.5. Development of operational chart using ANN

The new concept about treatment systems involves efficient operation as well as good design to achieve the desired goals. It should be understood that only efficiently operated plants can produce a minimum pollution load out of a good design. Consequently, process control has become an important issue in wastewater treatment systems. Expertise in process control of wastewater treatment systems needs specially automated control, which is a very attractive area of interest in the field. But the need for continuous measurement of system variables, which requires expert staff, again reduces efficiency. ANN models can be a solution to this problem in many aspects. ANN models are also good error predictors and can be used not only on behalf of a deterministic model, but can also be plugged into the system as an error predictor.

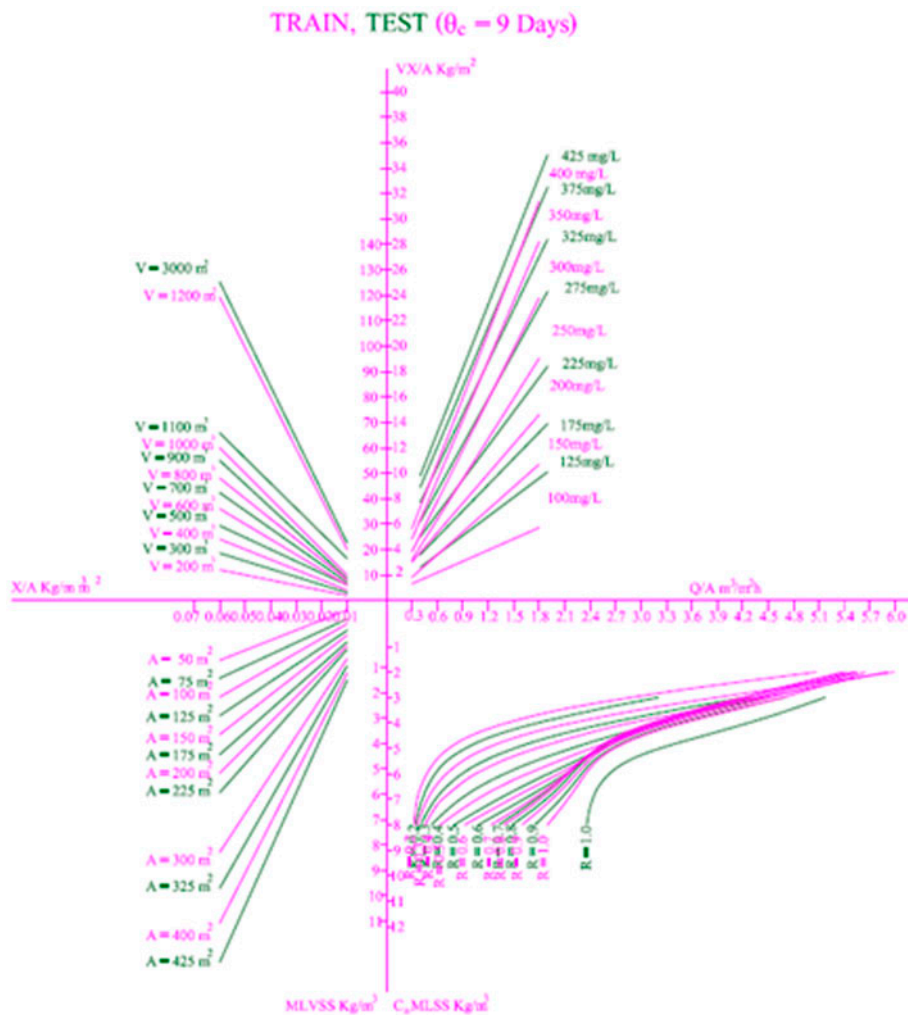


Fig. 10. Representative operational chart by superimposing ANN train and test data  $\theta_c = 9$  d.

In this study, a feed-forward algorithm was applied which consisted of one input layer, one hidden layer, and one output layer, all connected with no feed-forward connection, as discussed in Section 5. Volume of the reactor ( $V$ ), flow per unit area ( $Q/A$ ), initial substrate concentration ( $S_i$ ), initial MLSS concentration ( $C_0$ ), recycling ratio ( $R$ ), surface area of secondary clarifier ( $A$ ), and biomass per unit area of secondary clarifier ( $X/A$ ) were the input variables applied to the feed-forward NN, and the total biomass in the reactor per unit area of the secondary clarifier ( $VX/A$ ), ( $X/A$ ), MLVSS, and MLSS were the output variables. The number of neurons in the hidden layer was 0.05. With the experimental data of ( $Q/A$ ), ( $X/A$ ),  $V$ ,  $A$ ,  $C_0$ ,  $R$  as input and  $VX/A$ ,  $X$ ,  $Q/A$  as output, the ANN was trained for various  $\theta_c$  values (5, 7, 9, 11, 13 d). With the weights updated using experimental data, the ANN was trained with a new set of inputs ( $Q/A$ ), ( $V$ ), ( $A$ ), ( $C_0$ ), and  $R$ , which yielded the output of the ANN. A representative operational chart for 9 d given in Fig. 10 was obtained by superimposing the

training data and test data. Likewise, the representative operational chart for 7 d given in Fig. 11 was plotted by superimposing experimental, test, and training data to authenticate the meticulousness of the experimental and ANN results.

6.6. Interpretation from operational chart

Referring to Fig. 9, the operational chart for  $\theta_c = 5$  d and for an overflow rate ( $Q/A$ ) of  $1.2 \text{ m}^3/\text{m}^2 \text{ h}$ , influent substrate concentration of  $300 \text{ mg/L}$ , aerator volume ( $V$ ) of  $800 \text{ m}^3$ , settler area ( $A$ ) of  $150 \text{ m}^2$ , the MLVSS concentration, MLSS ( $C_0$ ) concentration, and recycle ratio ( $R$ ) were found to be  $5.5$ ,  $4.4$ , and  $0.8 \text{ g/L}$ , respectively. Assuming that the flow changed and the operating substrate concentration remained  $300 \text{ mg/L}$ , the new operating flow rate was found to be  $1.38 \text{ m}^3/\text{m}^2 \text{ h}$ . The corresponding values of MLVSS and MLSS were observed to be  $6.4$  and  $5.15 \text{ g/L}$ , which fall in the failure zone. In this case, the recycling ratio no longer saved the process from failure and control

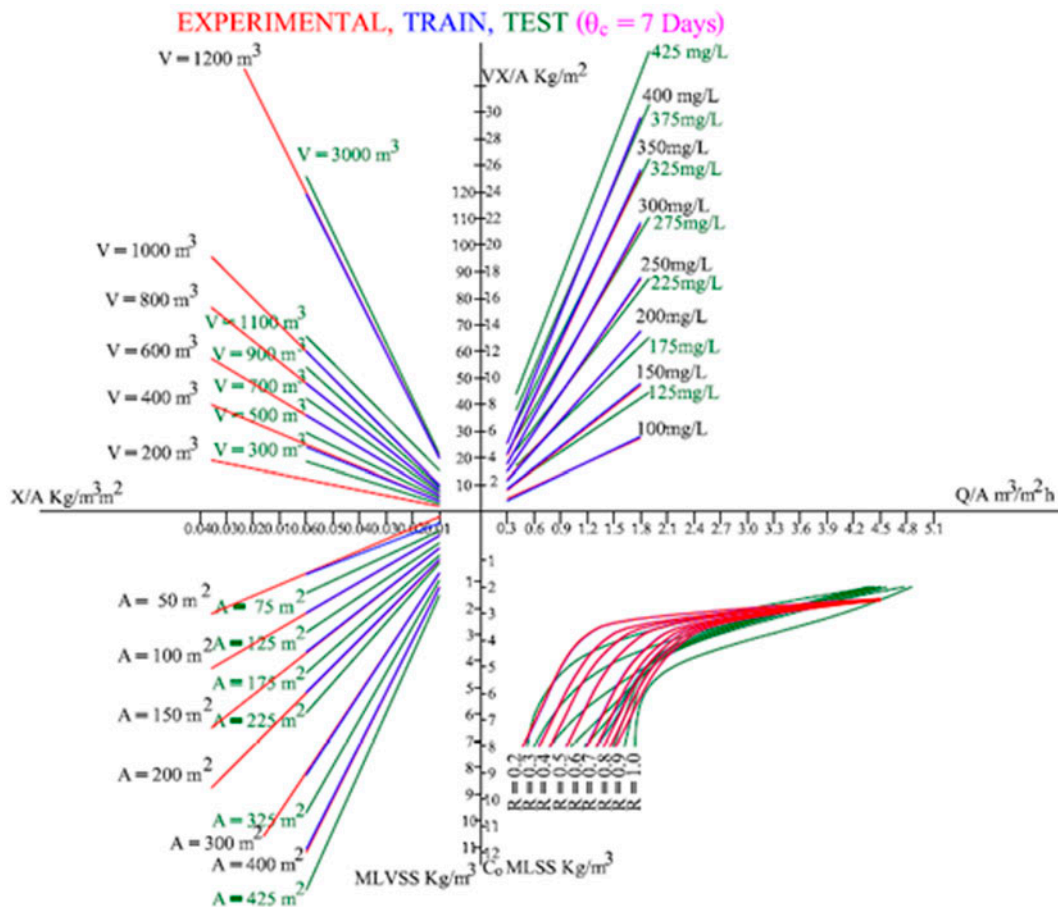


Fig. 11. Representative operational chart by superimposing experimental data, ANN train, and test data for  $\theta_c = 7$  d.

could be exercised by adjusting the  $\theta_c$  suitably. For an overflow rate of  $1.38 \text{ m}^3/\text{m}^2 \text{ h}$ , taking the MLSS concentration to be equal to  $C_0$  and compatible with the proper operation of the secondary clarifier at  $6.0 \text{ g/L}$ , the slope of the straight line (AB) gives an operating  $\theta_c$  of  $3.3 \text{ d}$  ( $0.6/0.18$ ). Hence, to maintain a  $\theta_c$  of  $3.3$ , wasting of MLSS from the reactor was to be done at the rate of  $242.42 \text{ m}^3/\text{d}$  (wasting rate  $Q_w = V/\theta_c$ ,  $800/3.3 = 242.42 \text{ m}^3/\text{d}$ ) instead of the designed wasting rate of  $800/5 = 160 \text{ m}^3/\text{d}$ .

## 7. Conclusion

A long-term research study was carried out in a South India-based paper and pulp mill WWTP using an aerobic treatment process with significant operating parameters and environmental conditions. This study was planned in such a way that the operational parameters were optimized in every stage of the treatment process so that the functioning of the WWTP should be cost-effective and the treatment efficiency more reliable. The following conclusions were drawn from the experimental investigations:

- (1) Microorganisms present in the paper and pulp mill wastewater were identified and the most efficient degraders were used for further studies.
- (2) The results obtained from the CCD experiments were fitted to a second-order polynomial equation to explain the dependence of microbial degradation on the medium components.
- (3) Treatment was carried out using coagulation\_flocculation process, and the data obtained were used by employing the Taguchi method and GRA to find the optimal conditions for removal of turbidity, COD, and TDS of paper mill wastewater as output responses. Thus, performance characteristics of coagulation\_flocculation process parameters are simultaneously improved together using GRA.
- (4) Further treatment of the paper and pulp mill wastewater was carried out with these optimized environmental factors and efficient microorganisms to design a secondary clarifier to develop operational charts.
- (5) Mathematical models were developed using ANN and SPSS software to predict the thickener area ( $A$ ) of the secondary settling tank, which was then used to draw the operational chart for steady state conditions.
- (6) With the help of the operational charts for a particular aerator volume ( $V$ ) and settler area ( $A$ ), it is possible:

- (a) to find the process parameters  $C_0$  and  $R$  for a given  $\theta_c$  for various flow rates and substrate concentrations,
  - (b) to evaluate the flexibility of the plant,
  - (c) to determine the operating conditions that lead to the process failure, and
  - (d) to estimate the  $\theta_c$  to be adjusted to prevent the failure.
- (7) When overflow rate ( $Q/A$ ) exceeds the maximum value, the process cannot be controlled by increasing the recycling ratio ( $R$ ). In this case, the mean cell residence time ( $\theta_c$ ) has to be adjusted to control the process failure.

## Acknowledgments

The authors are grateful to Seshasayee Paper and Boards Ltd., a South Indian paper and pulp mill for their helpfulness and overall technical assistance in undertaking the case study. We sincerely thank Dr Vidhya Iyer, Vellore, for helping with the manuscript preparation and for critical remarks.

## Nomenclature

$Y$	—	yield coefficient
$k_d$	—	endogenous decay coefficient ( $\text{d}^{-1}$ )
$\theta_c$	—	mean cell residence time (d)
$X$	—	concentration of volatile suspended solids in the reactor (mg/L)
$Q_w$	—	waste sludge flow rate (L/d)
$X_w$	—	concentration of volatile suspended solid in the waste (mg/L)
$Q$	—	flow rate (L/d)
$X_e$	—	concentration of volatile suspended solids in the effluent (mg/L)
$X_r$	—	concentration of volatile suspended solids in recycle line (mg/L)

## References

- [1] S. Sumathi, V. Phatak, Fungal treatment of bagasse based pulp and paper mill wastes, *Environ. Technol.* 20 (1999) 93–98.
- [2] A. Moharikar, H.J. Purohit, R. Kumar, Microbial population dynamics at effluent treatment plants, *J. Environ. Monit.* 7 (2005) 552–558.
- [3] H.E. Abd-Elsalam, Amr A. El-Hanafy, Lignin biodegradation with lygninolytic bacterial strain and comparison of *Bacillus* sp. isolated from Egyptian soil, *Am. Eurasian J. Agric. Environ. Sci.* 5(1) (2009) 39–44.
- [4] P. Singh, I.S. Thakur, Removal of color and de-toxification of pulp mill effluent by microorganisms in two step bioreactor, *J. Sci. Ind. Res.* 63(11) (2004) 944–948.

- [5] S. Singh, R. Chandra, D.K. Patel, M.M.K. Reddy, V. Rai, Investigation of the biotransformation of pentachlorophenol and pulp paper mill effluent decolorization by the bacterial strains in a mixed culture, *Bioresour. Technol.* 99 (2008) 5703–5709.
- [6] F. Wolfaardt, R.M. Toit, J. Grimbeek, Reduction of water consumption through closure of paper machine water loops: Impact of environmental changes on microbial fouling, in: *Proceedings of the Tappsa Berg Conference, Champagne Sports Resort* (2007).
- [7] G. Lindholm, Consumption of water in the pulp and paper industry, *Paper Technol.* 41(5) (2000) 57–60.
- [8] W.W. Eckenfelder, P. Grau, *The Activated Sludge Process Design and Control: Theory and Practice, Water Quality Management Library*, in: W.W. Eckenfelder, P. Grau (Eds.), vol. 1, Technomic Publishing Company Inc., Lancaster, PA, 1992.
- [9] M. Lerner, N. Stahl, N. Galil, Aerobic vs. anaerobic-aerobic biotreatment: Paper mill wastewater, *Environ. Eng. Sci.* 24(3) (2007) 277–285.
- [10] J. Zhang, F. Zhang, Y. Luo, H. Yang, A preliminary study on cactus as coagulant in water treatment, *Process. Biochem.* 41(3) (2006) 730–733.
- [11] A. Ndabigengesere, K.S. Narasiah, B.G. Talbot, Active agents and mechanism of coagulation of turbid waters using *Moringa oleifera*, *Water Res.* 29 (1995) 703–710.
- [12] R. Sanghi, B. Bhattacharya, A. Dixit, V. Singh, Ipomoea dasyperma seed gum: An effective natural coagulant for the decolorization of textile dye solutions, *J. Environ. Manage.* 81(1) (2006) 36–41.
- [13] S.A. Muyibi, L.M. Evison, Optimizing physical parameters affecting coagulation of turbid water with *Moringa oleifera* seeds, *Water Res.* 29(12) (1995) 2689–2695.
- [14] B. Meyssami, A. Kasaeian, Use of coagulants in treatment of olive oil wastewater model solutions by induced air flotation, *Bioresour. Technol.* 96(3) (2005) 303–307.
- [15] H. Ganjidoust, K. Tatsumi, T. Yamagishi, R.N. Gholian, Effect of synthetic and natural coagulant on lignin removal from pulp and paper wastewater, *Water Sci. Technol.* 35(2–3) (1997) 291–296.
- [16] R. Saraswathi, M.K. Saseetharan, Physicochemical parametric analysis of paper mill effluent using mixed cultures of bacteria and fungi, *J. Sci. Ind. Res.* 70 (2011) 1070–1078.
- [17] R. Saraswathi, M.K. Saseetharan, S. Suja, ANN based predictive model for performance evaluation of paper and pulp effluent treatment plant, *Int. J. Comput. Appl. Technol.* 45(4) (2012) 280–289.
- [18] R. Saraswathi, M.K. Saseetharan, Simultaneous optimization of multiple performance characteristics in coagulation-flocculation process for Indian paper industry wastewater, *Water Sci. Technol.* 66(6) (2012) 1231–1238.
- [19] G. Olosson, B. Newell, *Wastewater Treatment Systems*, IWA Publishing, London, 1999.
- [20] APHA, AWWA & WPCF, *Standard Methods for the Examination of Water and Wastewater*, twentieth ed., American Public Health Association, Washington, DC, 1995.
- [21] R. Saraswathi, M.K. Saseetharan, Effects of temperature and pH on floc stability and biodegradation in paper and pulp mill effluent, *J. Eng. Res. Stud.* 1(2) (2010) 166–176.
- [22] R. Saraswathi, M.K. Saseetharan, Investigation on microorganisms and their degradation efficiency in paper and pulp mill effluent, *J. Water Res. Prot.* 2 (2010) 660–664.
- [23] Z. Haiying, H. Hongtao, Z. Yi, C. Donghui, Q. Jingyu, Advanced treatment of the output-stream of biological leachate treatment by appropriate combination of coagulation/flocculation and oxidation, *Waste Manage. Res.* 30(1) (2012) 99–105.
- [24] S. Aber, D. Salari, M.R. Parsa, Employing the Taguchi method to obtain the optimum conditions of coagulation-flocculation process in tannery wastewater treatment, *Chem. Eng. J.* 162 (2010) 127–134.
- [25] E. Echeverría, A. Seco, J. Ferrer, Control of activated sludge settleability using preaeration and preprecipitation, *Water Res.* 27(2) (1993) 293–296.
- [26] A. Metcalf, E. Eddy, *Wastewater Engineering: Treatment and Reuse*, McGraw-Hill, Boston, MA, 2003.
- [27] G.W. Chen, I.L. Chang, W.T. Hung, D.J. Lee, Regimes for zone settling of waste activated sludges, *Water Res.* 30(8) (1996) 1844–1850.
- [28] R. Dupont, M. Henze, Modelling of the secondary clarifier combined with the activated sludge model No. 1, *Water Sci. Technol.* 25(6) (1992) 285–300.
- [29] D.S. Lee, C.O. Jeon, J.M. Park, K.S. Chang, Hybrid neural network modeling of a full-scale industrial wastewater treatment process, *Biotechnol. Bioeng.* 78 (6) (2002) 670–682.
- [30] Q. Zhang, S.J. Stanley, Real-time water treatment process control with artificial neural networks, *J. Environ. Eng.* 125(2) (1999) 153–160.
- [31] G. d’Antonio, P. Carbone, Activated sludge process control by behavior of secondary settling tanks, *Water Sci. Technol.* 19 (1987) 1207–1210.